Evidence of oxygen-stabilized hexagonal interstitial erbium in silicon

M. B. Huang* and X. T. Ren†
Department of Physics, State University of New York at Albany, Albany, New York 12222, USA
(Received 5 December 2002; revised manuscript received 18 April 2003; published 25 July 2003)

We report on the effects of codoped oxygen and thermal annealing on the evolution of lattice sites of erbium in silicon. At low concentrations of codoped impurities, it is evident that Er prefers occupation of the tetrahedral (*T*) interstitial site after Er ion implantation. Oxygen codoping can substantially populate implanted Er atoms onto the hexagonal (*H*) interstitial site. In the presence of oxygen, Er can be stabilized on the *H* site during annealing up to 900 °C. Also interesting is that post-implantation annealing can greatly promote occupation of the *H* site by Er in O-deficient Si, even though few Er atoms are found to be on the *H* site following Er ion implantation.

DOI: 10.1103/PhysRevB.68.033203 PACS number(s): 61.72.Tt, 68.55.Ln, 81.05.−t, 85.60.Bt

Doping erbium into silicon is a promising route for circumventing the problem of Si being an inefficient light emitter. The major advantage of Er-doped materials lies in the emission wavelength (1.54 μm) of the intrtra-$4f\,^4I_{13/2}$-$^4I_{15/2}$ transition of Er^{3+}, corresponding to the window of minimal loss for silica optical fibers used in telecommunications. It has been shown that the luminescence properties of Er can be significantly improved by adding other impurities in Er-doped Si, e.g., oxygen, being the one that gives rise to the most significant improvements.[1]

Despite extensive study, the role played by codoped O atoms is still not clear. Particularly, the correlation of various Er luminescence centers and their microstructures has not been established. Information about Er lattice locations in Si is very important for understanding the microstructures of Er-related centers. Previous theoretical investigations predicted the substitutional (*S*) site[2] or the tetrahedral (*T*) interstitial site[3] as the stable lattice location for isolated Er in Si. The effects of O codoping on Er lattice locations were also addressed theoretically, but no consensus has been reached. The simulations of Gan *et al.* suggested that O-related clusters with Er on the *S* site might be more stable than those involving Er on the *T* site.[1,4] Wan *et al.* predicted that the hexagonal (*H*) interstitial location should be the energetically favored site for Er in O-rich Si.[5] In contrast, a recent calculation proposed that the stable lattice location of Er would evolve from the *S* site at low O concentrations, to the *T* site at high O concentrations.[6] Experimentally, the lattice site of Er in Si was measured by charged particle channeling measurements, with results suggesting occupation of Er on the *S* site,[7,8] the *H* site,[9] or the *T* site,[10] respectively. The effects of codoped impurities on the lattice occupation of Er have not been clearly demonstrated in experiments.

The great disparities in experimental and theoretical results imply the great complexity of the issue and therefore warrant more investigations. In this Brief Report, we report on the effects of O codoping and post-implantation annealing on the occupation of Er lattice sites. Particularly, it is worth pointing out that our work differs from previous investigations in two respects: (1) the use of ion implantation and solid-phase epitaxial growth (SPEG) for incorporation of O in FZ-Si, allowing for an explicit study of the pure effects of O codoping, and (2) the use of hot implantation for Er incorporation in Si minimizing the influence of damage and extended defects on the determination of lattice sites. We performed ion channeling experiments to determine the occupancy of various lattice sites of Er in Si with and without codoped O. The samples were cut from an *n*-type (phosphorus-doped, 1500–2000 Ω cm) FZ-Si (100) wafer. The O-rich Si was prepared by O ion implantation into amorphous FZ-Si followed by SPEG. This processing allows us to eliminate the interference of other impurities (e.g., carbon) or the complication due to additional lattice damage caused by O ions if they were directly implanted into crystalline Si. A uniform amorphous Si layer of ∼300 nm thickness was first produced by 77-K Si ion implantation with multiple energies and doses. Oxygen ions of 50 keV ($R_p = 120 \pm 48$ nm) in energy were implanted into the amorphized Si layer to various doses between 10^{13} and 10^{15} cm^{-2}, producing O peak concentrations $\sim 10^{18}$–10^{20} cm^{-3}. The O-doped Si was regrown via SPEG at 600 °C for 6 h, resulting in a crystal quality as good as virgin Si (from the perspective of ion channeling). Finally, the O-doped samples along with an O-deficient (FZ-Si) control sample were implanted with 380-keV Er ions ($R_p = 127 \pm 25$ nm) to a dose of 5×10^{14} cm^{-2}. The Er ion implantation was conducted at

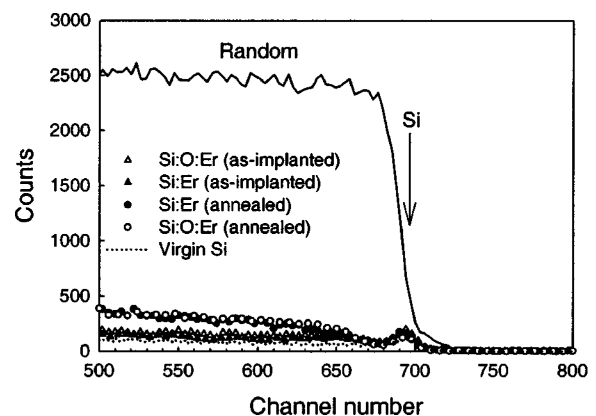

FIG. 1. Rutherford backscattering (RBS) and channeling spectra along the ⟨110⟩ direction for O-deficient and O-doped (O dose: 5×10^{14} cm^{-2}) Si samples following Er implantation and thermal annealing at 900 °C, respectively. Note that the Si signals for the O-deficient and O-rich samples are almost identical.

 ©2003 The American Physical Society

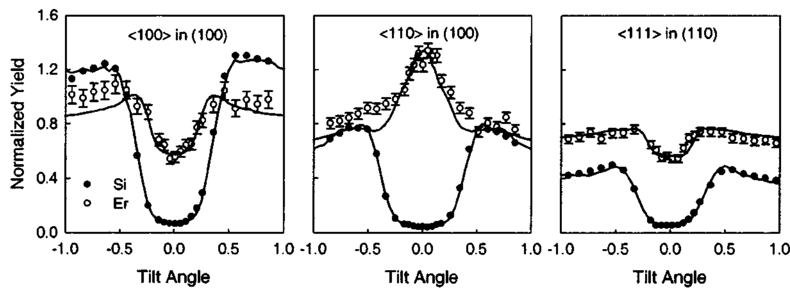

FIG. 2. Normalized RBS yield as a function of tilt angles along three major crystal directions in the O-deficient Si following Er ion implantation. The solid lines represent the Monte Carlo simulation results.

300 °C, which helps suppress the formation of a highly damaged layer in Si. Before ion implantation, samples were rinsed with dilute hydrofluoric acid to remove the surface native oxide, preventing the unintentional incorporation of excess O due to recoil processes. The Er-implanted samples were further subjected to furnace annealing in a temperature range of 500–1200 °C for 30 min with a flowing nitrogen gas. Rutherford backscattering and channeling experiments were performed using a 2.5-MeV He^+ beam. It should be pointed out that the processes involving crystal amorphization via Si self-implantation followed by SPEG, excluding the step for O incorporation, do not cause any measurable effects on the occupation of Er lattice sites.

After Er ion implantation, the crystals were slightly damaged in the region corresponding to the projected range of implanted Er ions (Fig. 1), e.g., the minimum yield $\chi_{\min}$ of Si in the damaged region (between channels 650 and 660), being ~5% for both O-deficient and O-doped Si samples. After annealing between 700 and 900 °C, a small increase of dechanneling yields was detected in the region corresponding to the end of Er ion range, indicating the formation of a layer of extended defects, commonly observed following post-implantation annealing.[1,9,11] These extended defects disappear as annealing temperatures ⩾1000 °C. The channeling spectra show almost identical Si signals for both O-doped and O-deficient Si, indicating that the conditions for ion channeling in O-deficient and O-doped Si samples are virtually the same.

The normalized yields of Er (energy window: channels 1100–1150) and Si (energy window: channels 650–660) as a function of tilt angle along three low-index crystalline directions (⟨100⟩, ⟨110⟩, and ⟨111⟩) were monitored (Figs. 2 and 3). To determine the percentage fraction of Er atoms on different lattice sites, we conducted Monte Carlo simulations using the FLUX7 code.[12] The calculated angular scan curves for the *H*-site and *T*-site Er have been presented in our previous work.[13] They are similar in the ⟨110⟩ direction—i.e., showing peaks with intensity above 1.0 in the center of the channel—but are dramatically different in the other two directions (⟨100⟩ and ⟨111⟩). Along the ⟨100⟩ and ⟨111⟩ directions, the *T*-site atoms are shadowed by substitutional host atoms, resulting in the corresponding angular scan curves same as those of the *S*-site or Si host atoms. The *H*-site atoms are viewed as large displacement atoms along ⟨100⟩ or located at the center of the channel along ⟨111⟩, leading to the corresponding normalized yields higher than the case (i.e., 1.0) for atoms on the random (*R*) site. The angular scan curves for the *S*-site Er along three directions are exactly the same as those of the host (Si) atoms. Our experimental data for the ⟨110⟩ scan show a pronounced peak with the normalized intensity well above the unity. This strongly indicates the occupation of *T* and/or *H* interstitial sites by most Er atoms, because flux peaking cannot be observed in the ⟨110⟩ direction if Er were to occupy sites other than the *T* and/or *H* site. As a result, occupation of the *S* site, the corner (*C*) site, and the bonding (*B*) or antibonding (AB) site, etc., by a significant amount (>5%) of Er can be easily ruled out. The resultant peak concentration of Er in our experiment is expected to be above the solubility of Er in Si, and therefore the low symmetry or the *R* site corresponding to the phase of Er precipitates was considered in addition to the *T* and *H* sites in our simulations to fit the experimental angular scan curves. As compared to the case where ion beams are well aligned in the crystal direction, the scattering yields resulted from an off-center incidence could be more susceptible to crystal distortions induced by incorporation of impurities. Consequently, an important criterion for the best fit of data is whether the data points in the center region of the channel can be accounted for by the calculated angular scan curves for all three crystal directions. The tolerance of the extracted site occupancies was estimated by varying their fitting values until the calculated normalized yields (in the region close to the channel center) exceed the range set by the uncertainty of the corresponding data points.

Following Er ion implantation, the above-described fitting procedure indicates that a large fraction (~45%) of Er is

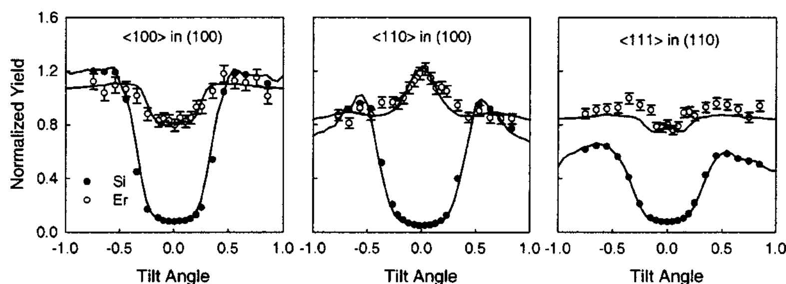

FIG. 3. Normalized RBS yield as a function of tilt angles along three major crystal directions in the O-rich Si (O dose: 5×10^{14} cm^{-2}) following Er ion implantation. The solid lines represent the Monte Carlo simulation results.

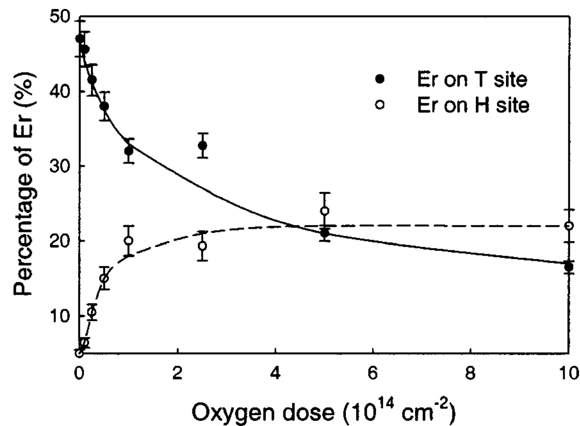

FIG. 4. Percentage fraction of Er on the T and H sites as functions of codoped O doses. The lines are drawn to guide the eyes.

located at near-T sites (0.25 Å from the T site toward the H site) and few Er atoms (<5%) on the H site in the O-deficient Si. A similar conclusion has also been drawn in the work of Wahl *et al.*[10] Both our work and the work of Wahl *et al.* may provide evidence supporting the calculation of Needles *et al.*,[3] which proposes the T site as the equilibrium lattice site for Er in Si without any codopants. In addition, our data show that codoping O in Si:Er results in a small reduction of the normalized yield in the center of ⟨110⟩ channel and a significant enhancement of the normalized yield in the ⟨100⟩ and ⟨111⟩ directions. Obviously, the possibility for a large amount of Er (>5%) occupying the S site in the presence of O can be eliminated, since the S-site Er would give rise to a substantial decrease in the normalized yields for all three directions, contradicting our observations. For Si:Er codoped with O to the dose of 5×10^{14} cm^{-2}, the fitting results indicate that the fraction for T-site Er is reduced to ~20% and the fraction for H-site Er enhanced to ~25%, as opposed to the case without O codoping. Figure 4 shows the occupancies of H-site and T-site Er at various codoped O contents following Er ion implantation at 300 °C. As seen, codoping O in Si:Er leads to a conversion in the occupation of Er lattice locations from the T site to the H site. At low O concentrations, more Er atoms occupy the T site than the H site, but the concentration of H-site Er exceeds that of T-site Er as the codoped O dose $\geqslant 5\times10^{14}$/cm^2. The H-site concentration increases rapidly at low O doses and reaches a saturation beyond the O dose of 10^{14} cm^{-2}. This seems to suggest that about one O atom may be required to populate one Er atom onto the H site.

The enhancement in the H-site occupation resulted from O codoping suggests that Er and O can interact strongly with each other, possibly leading to the formation of Er-O complexes that may be stabilized as the involved Er atoms are placed on the H site. Our observations of O codoping effects on Er lattice site occupation seem to support the theoretical work of Wan *et al.*,[5] which predicts that the energetically stable location for Er in Si would evolve from the T site in the case without codopants, to the H site as O is incorporated. We have also examined thermal annealing effects on the occupation of Er lattice sites. The data show that Er-O complexes, which are formed during ion implantation processes, can be stable against thermal annealing up to 900 °C. As shown in Fig. 5, the concentration of H-site Er in the O-rich Si (codoped O dose: 5×10^{14} cm^{-2}) sample remains virtually unchanged after annealing up to 900 °C. The annealing behaviors for H-site Er may be related to the annealing effects on photoluminescence intensity from the Si:Er:O system. It has been generally observed in previous optical investigations that the Er luminescence intensity decreases sharply as the annealing temperature is elevated above 900 °C and the drop of optical activities was ascribed to the dissociation of Er-O complexes.[1] Our annealing study may provide additional evidence for the breakup of Er-O complexes at high annealing temperatures. As Er-O complexes are dissociated, Er is expected to become isolated from O and precipitation of Er should be enhanced. This is indeed reflected in our observations showing a reduction of H-site Er concentrations accompanied by an increase of the concentration of R-site Er in the O-rich Si, following annealing at temperatures >900 °C.

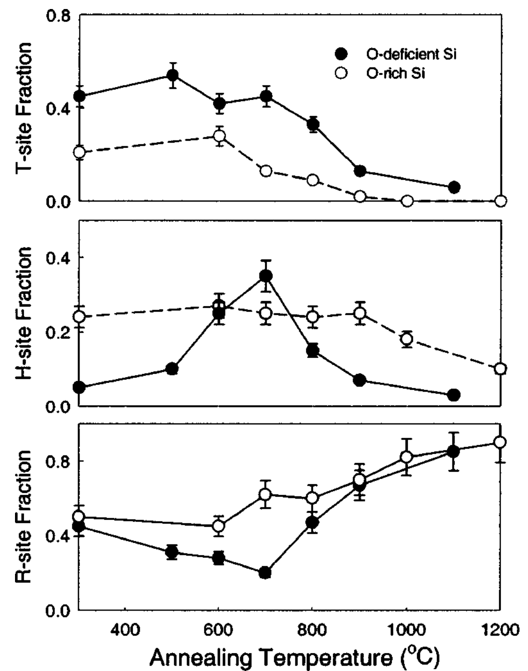

FIG. 5. Occupancies of Er on different lattice sites after post-implantation annealing. The values at 300 °C correspond to the case following Er implantation (prior to annealing).

Another interesting feature of our data shows that the fraction of H-site Er in the O-deficient Si can be considerably enhanced after annealing, although few Er atoms appear to be on the H site following Er implantation. The fraction of H-site Er in the O-deficient Si reaches a maximum of ~35% at 700 °C as opposed to the initial value of less than 5% prior to annealing. Unlike the case with O codopants, the fraction of H-site Er in the O-deficient Si drops rapidly at temperatures higher than 700 °C, e.g., only about 7% of Er atoms occupying the H site after annealing at 900 °C. We speculate that interactions of Er with point defects (most likely Si vacancies), released during post-implantation annealing, could be responsible for the appearance of H-site Er in the O-deficient Si. At low temperatures (<700 °C), vacancies are

emitted as a result of the dissociation of vacancy clusters and agglomerates.[14,15] Our data indicate that low-temperature (<700 °C) annealing of the O-deficient Si decreases the fraction of randomly located Er atoms, but the fraction of *T*-site Er is not altered. This may suggest that point defects are likely coupling to those low-symmetry Er atoms, resulting in the formation of defect complexes with Er on the *H* site. As annealing temperatures are above 700 °C, a supersaturation of Si interstitials should be present in the sample,[16] resulting in a vacancy concentration even lower than the equilibrium case and thus a reduced efficiency for Er to occupy the *H* site in the O-deficient Si.

In summary, we have shown the effects of oxygen codoping and post-implantation annealing on Er lattice locations in Si. At low O concentrations, the *T* interstitial site is the energetically favored position for Er in Si following implantation, but occupation of the *H* interstitial site by Er can be promoted after post-implantation annealing. The appearance of *H*-site Er in O-deficient Si after annealing may be related to the coupling between Er and point defects. At high O concentrations, our data suggest that implanted Er atoms prefer occupation of the *H* site over the *T* site. The incorporation of O in Si:Er is demonstrated to stabilize Er on the *H*-site Er during ion implantation and subsequent annealing up to 900 °C. These results may also provide insights into the understanding of large discrepancies in reports on Er lattice locations in Si, implying that impurity species, trap concentrations, and defect recombination and production could be important factors determining Er lattice locations in Si.

*Author to whom correspondence should be addressed. Electronic address: mhuang@csc.albany.edu

†On leave from the Institute of Heavy Ion Physics, Peking University, China.

[1] J. Michel, L. V. C. Assali, M. T. Morse, and L. C. Kimerling, in *Light Emission in Silicon: From Physics to Devices*, edited by D. J. Lockwood, *Semiconductors and Semimetals* Vol. 49 (Academic, San Diego, 1998), p. 111.

[2] C. Delerue and M. Lannoo, Phys. Rev. Lett. **67**, 3006 (1991).

[3] M. Needles, M. Schulter, and M. Lannoo, Phys. Rev. B **47**, 15 533 (1993).

[4] F. Gan, L. V. C. Assali, and L. C. Kimerling, Mater. Sci. Forum **196–201**, 579 (1995).

[5] J. Wan, Y. Ling, Q. Sun, and X. Wang, Phys. Rev. B **58**, 10 415 (1998).

[6] A. G. Raffa and P. Ballone, Phys. Rev. B **65**, 121309 (2002).

[7] Y. S. Tang, J. Zhang, K. C. Heasman, and B. J. Sealy, Solid State Commun. **72**, 991 (1989).

[8] C. Clerc, H. Bernas, J. Chaumont, P. Boucaud, F. Julien, and J. M. Lourtioz, Thin Solid Films **294**, 223 (1997).

[9] A. Kozanecki, J. Kaczanowski, R. Wilson, and B. J. Sealy, Nucl. Instrum. Methods Phys. Res. B **118**, 709 (1996).

[10] U. Wahl, A. Vantomme, J. De Wachter, R. Moons, G. Langouche, and J. G. Marques, Phys. Rev. Lett. **79**, 2069 (1997).

[11] F. Priolo, S. Coffa, G. Franzò, C. Spinella, A. Carnera, and V. Bellani, J. Appl. Phys. **74**, 4936 (1993).

[12] P. J. M. Smulders and D. O. Boerma, Nucl. Instrum. Methods Phys. Res. B **29**, 471 (1987).

[13] M. B. Huang and X. T. Ren, Appl. Phys. Lett. **81**, 2734 (2002).

[14] M. B. Huang, U. Myler, P. J. Simpson, and I. V. Mitchell, J. Appl. Phys. **87**, 7685 (2000).

[15] P. Pellegrino, P. Lévêque, J. Lalita, A. Hallén, C. Jagadish, and B. G. Svensson, Phys. Rev. B **64**, 195211 (2001).

[16] P. A. Stolk, H.-J. Gossmann, D. J. Eaglesham, D. C. Jacobson, C. S. Rafferty, G. H. Gilmer, M. Jaraíz, J. M. Poate, H. S. Luftman, and T. E. Haynes, J. Appl. Phys. **81**, 6031 (1997).